BULLETIN OF THE POLISH ACADEMY OF SCIENCES
TECHNICAL SCIENCES, Vol. 68, No. 5, 2020
DOI: 10.24425/bpasts.2020.134654

SPECIAL SECTION

Nonadaptive estimation of the rotor speed in an adaptive full order observer of induction machine

M. MORAWIEC* and P. KROPLEWSKI

Gdańsk University of Technology, Faculty of Electrical and Control Engineering, ul. Narutowicza 11/12, 80-233, Gdańsk

Abstract. The article proposes a new method of reproducing the angular speed of the rotor of a cage induction machine designed for speed observers based on the adaptive method. In the proposed solution, the value of the angular speed of the rotor is not determined by the classical law of adaptation using the integrator only by an algebraic relationship. Theoretical considerations were confirmed by simulation and experimental tests.

Key words: observers, induction machines, speed estimation, adaptive full order observer.

1. Introduction

Squirrel-cage induction machines (IM) are widely used in drive systems due to their relatively simple construction and satisfactory dynamic properties. Often, in drive systems, to increase reliability, in addition to the speed sensor, an estimator is used to reproduce the value of the rotor angular speed or position.

Methods of the rotor angular speed reproduction can be divided into three main groups [1]: physical, algorithmic, and neural network. One of the most used methods is algorithmic, which is characterized by the fact that the speed observer is based on the mathematical model of a machine. Algorithmic methods include the state observer (full and reduced order), e.g. [2], the full-order adaptive observer AFO [3–5], Kalman filter [6], structures based on sliding technique [7, 8] or MHE approach [9].

Due to the simplicity of implementation and good properties, a large group are the structures following the reference model MRAS [10, 11] in which the value of the rotor angular speed is obtained by means of the classic adaptation law, using an integrator or PI – proportional integration controller.

Another way to reproduce the angular rotor speed is to extend the mathematical model of the machine with an additional state variable based on it, as well as an appropriate algebraic transformation, determining the value. A nonadaptive method is presented for example in [12] and generalized for the n-phase machines in [13]. The speed estimation method proposed in [12, 13] is characterized by a large number of observer tuning gains and a complicated form of stabilizing functions. In [14] the structure of the observer is presented in which stabilizing functions were obtained based on the backstepping method, which significantly reduced the number of tuning gains compared to [13]. However, the observer model was extended by an additional integrator.

The main problem occurring in the sensorless control structure is the stable work of a drive system in the range of very low rotor speeds (less than 10-20 rpm), the operation near to zero or the zero rotor angular speed and a set value of load torque in the range of motor and, above all, in the regenerating mode [3, 4, 7, 8, 11, 12, 15].

This paper proposes a method of estimating the angular rotor speed, which can be applied to the structures of observers AFO [3–5, 11] as well as MRAS [10, 11, 16], consisting of determining the speed value from an algebraic relationship (nonadaptive without using an integrator). In addition, a method of robust classical adaptation law (with integrator) for the range of motor and regenerating operation as well as rotor speed command less than 0.1 p.u. was proposed. All the presented theoretical issues were confirmed by the simulation and experimental research on a 5.5 kW machine.

2. Mathematical model of induction machine

A squirrel-cage induction machine can be represented by the differential equations for the stator current vector and the rotor flux [12–14, 17]:

$$\frac{\mathrm{d}\boldsymbol{i}_s}{\mathrm{d}\tau} = a_1\boldsymbol{i}_s + a_2\boldsymbol{\psi}_r + ja_3\omega_r\boldsymbol{\psi}_r + a_4\boldsymbol{u}_s\,, \tag{1}$$

$$\frac{\mathrm{d}\boldsymbol{\psi}_r}{\mathrm{d}\tau} = a_5\boldsymbol{\psi}_r + j\omega_r\boldsymbol{\psi}_r + a_6\boldsymbol{i}_s\,, \tag{2}$$

and the equation of motion

$$\frac{\mathrm{d}\omega_r}{\mathrm{d}\tau} = \frac{1}{J}\left(T_e - T_L\right), \tag{3}$$

*e-mail: marcin.morawiec@pg.edu.pl

Manuscript submitted 2020-01-09, revised 2020-04-03, initially accepted for publication 2020-04-19, published in October 2020

where $\boldsymbol{i}_s$, $\boldsymbol{u}_s$, $\boldsymbol{\psi}_r$ are the vectors of current, stator voltage and rotor flux, respectively, and the following designations have been introduced:

$$a_1 = -\frac{R_s L_r^2 + R_r L_m^2}{L_r w_\sigma}, \qquad a_2 = \frac{R_r L_m}{L_r w_\sigma}, \qquad a_3 = \frac{L_m}{w_\sigma}, \qquad a_4 = \frac{L_r}{w_\sigma}, \tag{4}$$

$$a_5 = -\frac{R_r}{L_r}, \qquad a_6 = \frac{R_r L_m}{L_r}, \qquad w_\sigma = L_r L_s - L_m^2. \tag{5}$$

At the design stage of the control system, it is assumed that the machine parameters are known and unchanging in time, and the components of the stator current vector $i_{s\alpha}$, $i_{s\beta}$ as well as the components of the stator voltage vector $u_{s\alpha}$, $u_{s\beta}$ are quantities known or available for measurement, $\psi_{r\alpha}$, $\psi_{r\beta}$ are components of the rotor flux vector, ω_r is the value of angular speed.

3. Full-order speed observer

The mathematical model of IM can be presented in a generalized form [1–5]:

$$\dot{\boldsymbol{x}} = \boldsymbol{A}\,\boldsymbol{x} + \boldsymbol{B}\,\boldsymbol{u}, \tag{6}$$

$$\boldsymbol{y} = \boldsymbol{C}\,\boldsymbol{x}, \tag{7}$$

where $\boldsymbol{x}$ is the vector of state variables, $\boldsymbol{u}$ is the vector of controls and $\boldsymbol{A}$, $\boldsymbol{B}$, $\boldsymbol{C}$ contain the constant parameters of IM.

The full-order observer for (6)–(7) can be determined by the following differential equations:

$$\dot{\hat{\boldsymbol{x}}} = \boldsymbol{A}\hat{\boldsymbol{x}} + \boldsymbol{B}\,\boldsymbol{u} + \boldsymbol{G}\tilde{\boldsymbol{x}}, \tag{8}$$

$$\hat{\boldsymbol{y}} = \boldsymbol{C}\hat{\boldsymbol{x}}, \tag{9}$$

where $\boldsymbol{G}$ is the matrix which contains the observer tuning gains and

$$\tilde{\boldsymbol{x}} = \hat{\boldsymbol{i}}_s - \boldsymbol{i}_s. \tag{10}$$

Using (6), (7) it is possible to determine the dynamics of the observer estimation error:

$$\dot{\tilde{\boldsymbol{x}}} = (\boldsymbol{A} + \boldsymbol{G}\,\boldsymbol{C})\tilde{\boldsymbol{x}}. \tag{11}$$

Assuming that the eigenvalues of the matrix $\boldsymbol{F} = \boldsymbol{A} + \boldsymbol{G}\,\boldsymbol{C}$ have the negative values and for $t \to \infty$ the estimation error of state variables $\tilde{\boldsymbol{x}}(t) \to 0$ decays to zero and according to Lyapunov theorem, the observer structure will be asymptotical stable:

$$\dot{\tilde{\boldsymbol{x}}} = e^{\boldsymbol{F}t}\tilde{\boldsymbol{x}}(t). \tag{12}$$

Considering the observer model in the coordinate system $(\alpha\beta)$ connected to the stator, the following can be obtained [1–5]:

$$\frac{\mathrm{d}\hat{i}_{s\alpha}}{\mathrm{d}\tau} = a_1\hat{i}_{s\alpha} + a_2\hat{\psi}_{r\alpha} + a_3\hat{\omega}_r\hat{\psi}_{r\beta} + a_4 u_{s\alpha} + v_\alpha, \tag{13}$$

$$\frac{\mathrm{d}\hat{i}_{s\beta}}{\mathrm{d}\tau} = a_1\hat{i}_{s\beta} + a_2\hat{\psi}_{r\beta} - a_3\hat{\omega}_r\hat{\psi}_{r\alpha} + a_4 u_{s\beta} + v_\beta, \tag{14}$$

$$\frac{\mathrm{d}\hat{\psi}_{r\alpha}}{\mathrm{d}\tau} = a_5\hat{\psi}_{r\alpha} - \hat{\omega}_r\hat{\psi}_{r\beta} + a_6\hat{i}_{s\alpha} + v_{\psi\alpha}, \tag{15}$$

$$\frac{\mathrm{d}\hat{\psi}_{r\beta}}{\mathrm{d}\tau} = a_5\hat{\psi}_{r\beta} + \hat{\omega}_r\hat{\psi}_{r\alpha} + a_6\hat{i}_{s\beta} + v_{\psi\beta}, \tag{16}$$

where $v_{\alpha,\beta}$ and $v_{\psi\alpha,\beta}$ are stabilizing functions introduced to the structure.

The observer structure (13)–(16) will be asymptotical stable if following Lyapunov function:

$$V_1 = \frac{1}{2}\left(\tilde{i}_{s\alpha}^2 + \tilde{i}_{s\beta}^2 + \tilde{\psi}_{r\alpha}^2 + \tilde{\psi}_{r\beta}^2\right) > 0, \tag{17}$$

and their derivative is negative determined:

$$\dot{V}_1 = \dot{\tilde{i}}_{s\alpha} + \dot{\tilde{i}}_{s\beta} + \dot{\tilde{\psi}}_{r\alpha} + \dot{\tilde{\psi}}_{r\beta} \le 0. \tag{18}$$

Model of estimation errors for (13)–(16) has the following form:

$$\frac{\mathrm{d}\tilde{i}_{s\alpha}}{\mathrm{d}\tau} = a_1\tilde{i}_{s\alpha} + a_2\tilde{\psi}_{r\alpha} + a_3\left(\tilde{\omega}_r\hat{\psi}_{r\beta} + \hat{\omega}_r\tilde{\psi}_{r\beta} - \tilde{\omega}_r\tilde{\psi}_{r\beta}\right) + v_\alpha, \tag{19}$$

$$\frac{\mathrm{d}\tilde{i}_{s\beta}}{\mathrm{d}\tau} = a_1\tilde{i}_{s\beta} + a_2\tilde{\psi}_{r\beta} - a_3\left(\tilde{\omega}_r\hat{\psi}_{r\alpha} + \hat{\omega}_r\tilde{\psi}_{r\alpha} - \tilde{\omega}_r\tilde{\psi}_{r\alpha}\right) + v_\beta, \tag{20}$$

$$\frac{\mathrm{d}\tilde{\psi}_{r\alpha}}{\mathrm{d}\tau} = a_5\tilde{\psi}_{r\alpha} - \left(\tilde{\omega}_r\hat{\psi}_{r\beta} + \hat{\omega}_r\tilde{\psi}_{r\beta} - \tilde{\omega}_r\tilde{\psi}_{r\beta}\right) + a_6\tilde{i}_{s\alpha} + v_{\psi\alpha}, \tag{21}$$

$$\frac{\mathrm{d}\tilde{\psi}_{r\beta}}{\mathrm{d}\tau} = a_5\tilde{\psi}_{r\beta} + \left(\tilde{\omega}_r\hat{\psi}_{r\alpha} + \hat{\omega}_r\tilde{\psi}_{r\alpha} - \tilde{\omega}_r\tilde{\psi}_{r\alpha}\right) + a_6\tilde{i}_{s\beta} + v_{\psi\beta}, \tag{22}$$

where

$$\tilde{\omega}_r = \hat{\omega}_r - \omega_r, \qquad \tilde{\psi}_{r\alpha,\beta} = \hat{\psi}_{r\alpha,\beta} - \psi_{r\alpha,\beta}, \qquad \tilde{i}_{s\alpha,\beta} = \hat{i}_{s\alpha,\beta} - i_{s\alpha,\beta}. \tag{23}$$

The observer structure (13)–(16) will be stable if the Lyapunov theorem is satisfied. According to the procedure of determining the adaptive control law, the Lyapunov function (17) should be extended to the form:

$$V = V_1 + \frac{1}{2\gamma}\tilde{\omega}_r^2. \tag{24}$$

By using (19)–(22), the derivative of the function (24) is as follows

$$\dot{V} = a_5\left(\tilde{\psi}_{r\alpha}^2 + \tilde{\psi}_{r\beta}^2\right) + \tilde{\omega}_r\left(\frac{1}{\gamma}\dot{\tilde{\omega}}_r - a_3\hat{\psi}_{r\alpha}\tilde{i}_{s\beta} + a_3\hat{\psi}_{r\beta}\tilde{i}_{s\alpha}\right) \le 0, \tag{25}$$

wherein (13)–(16) the observer stabilizing functions are introduced, which for $\dot{V} \leq 0$ should be taken:

$$v_\alpha = -c_\alpha \tilde{i}_{s\alpha}, \quad v_\beta = -c_\alpha \tilde{i}_{s\beta}, \tag{26}$$

$$v_{\psi\alpha} = -c_{\psi 1}\tilde{i}_{s\alpha} + c_\psi \hat{\omega}_r \tilde{i}_{s\beta}, \quad v_{\psi\beta} = -c_{\psi 1}\tilde{i}_{s\beta} - c_\psi \hat{\omega}_r \tilde{i}_{s\alpha}, \tag{27}$$

where it is assumed that $\tilde{\psi}_{r\alpha,\beta} \approx 0$, $c_\alpha = f(a_1) > 0$, $c_\psi = f(a_3) > 0$, whereas $c_{\psi 1} \geq 0$, $a_5 < 0$.

The value of rotor speed can be reproducing from an adaptive mechanism by using the integrator in the same as in [3] but in the stationary coordinate system $(\alpha\beta)$:

$$\frac{\mathrm{d}\tilde{\omega}_r}{\mathrm{d}\tau} = -\gamma a_3 \left(\tilde{i}_{s\alpha}\hat{\psi}_{r\beta} - \tilde{i}_{s\beta}\hat{\psi}_{r\alpha}\right), \tag{28}$$

assuming that $\dot{\omega}_r = 0$ and $\tilde{\omega}_r = \hat{\omega}_r$.

Reconstruction of rotor speed from the classic law of adaptation (28) can lead to a deterioration of properties of the observer structure due to the open-loop of an integrator, as noted in [18]. Therefore, the following feedback law is proposed in this paper:

$$\frac{\mathrm{d}\hat{\omega}_r}{\mathrm{d}\tau} = -\gamma a_3 \left(\tilde{i}_{s\alpha}\hat{\psi}_{r\beta} - \tilde{i}_{s\beta}\hat{\psi}_{r\alpha} + \gamma_1 \hat{\omega}_r\right), \tag{29}$$

where $(\gamma,\ \gamma_1) > 0$.

The coupling $(-\gamma_1 \hat{\omega}_r)$ leads to improved system stability. However, it does not immunize the observer, which may be susceptible to, e.g. external disturbances that were not considered at the design stage (variation of machine parameters during operation and others). Therefore, the author of this paper would like to propose three different approaches to rotor speed estimation. The basis for the synthesis of the structure of the speed observer is the mathematical model of the induction machine determined by space vectors in the stationary coordinate system $(\alpha\beta)$.

Proposition 1. Taking into account any two vectors defined in the reference system $(\alpha\beta)$, which are state estimates in the system (8), (9) or estimation errors, between which the following relationships occur:

$$\vec{a} \times \vec{b} \neq 0, \tag{30}$$

$$\vec{a} \cdot \vec{b} \cong 0, \tag{31}$$

where

$\vec{a} \times \vec{b}$ means vector product of two vectors,

$\vec{a} \cdot \vec{b}$ means a scalar product,

the law of adaptation from which the rotor angular speed is reconstructed can be generalized to the form:

$$\frac{\mathrm{d}\hat{\omega}_r}{\mathrm{d}\tau} = \gamma\left(\vec{a} \times \vec{b} - \gamma_1 \hat{\omega}_r\right), \tag{32}$$

where $\left(\vec{a},\ \vec{b}\right)$ is the selected pair of two vectors in the system.

The sign of expression (32) as well as additional parameters that may appear in (32) depend on the designed structure and directly result from the Lyapunov function from which the stability of the observer is examined.

The proof of Proposition 1 can be presented assuming that the possible pairs of vectors in the case of a squirrel-cage induction machine can be: $\left(\vec{\tilde{i}}_s,\ \vec{\hat{\psi}}_r\right)$, $\left(\vec{\tilde{i}}_s,\ \vec{\tilde{\psi}}_r\right)$, while the flux error vector module is not available in terms of measurement, thus $\left|\vec{\tilde{\psi}}_r\right| = 0$. Considering the first pair of vectors $\left(\vec{\tilde{i}}_s,\ \vec{\hat{\psi}}_r\right)$, the expression (3) for the machine motion equation is obtained, assuming that $T_L = 0$ and J is a known value. The observer structure is tuned by this value. For the second pair of vectors $\left(\vec{\tilde{i}}_s,\ \vec{\hat{\psi}}_r\right)$, the form of (28) is obtained. For the pair of vectors $\left(\vec{\tilde{i}}_s,\ \vec{\hat{\psi}}_r\right)$ the ideal case was assumed, in which it was assumed that the machine parameters are known and $\vec{a} \cdot \vec{b} = 0$ (vectors $\left(\vec{a},\ \vec{b}\right)$ are perpendicular). In practice, the scalar product of two selected vectors $\left(\vec{a},\ \vec{b}\right)$ (e.g. $\left(\vec{\tilde{i}}_s,\ \vec{\hat{\psi}}_r\right)$) does not equal zero but may be close to this value. The reason for this are the disturbances introduced into the observer structure related to the uncertainty of parameters, accuracy of measurements, accuracy of the voltage or current generated by the power electronic converter and discretization errors [19]. Therefore, the robust law of adaptation in addition to feedback $(\gamma_1 \hat{\omega}_r)$ in the integrator structure should be based not only on the vector product but also on the scalar product.

Proposition 2. A robust law of adaptation can be obtained by introducing feedback, which makes the integrator (32) have the following form:

$$\frac{\mathrm{d}\hat{\omega}_r}{\mathrm{d}\tau} = \gamma\left(\vec{a} \times \vec{b} - \gamma_1 \hat{\omega}_r \left(\vec{a} \cdot \vec{b}\right)\right). \tag{33}$$

Considering the ideal case, in which the vectors are perpendicular to each other, the form of (32) (for $\gamma = 0$ that is classical control law) is obtained, while in the case when $\vec{a} \cdot \vec{b} \neq 0$, additional feedback arises compensating for uncertainties interference and improving the robustness of observer system.

The adaptation mechanism (29) in the considered case including (33) has the form:

$$\frac{\mathrm{d}\hat{\omega}_r}{\mathrm{d}\tau} = -\gamma a_3 \left(\tilde{i}_{s\alpha}\hat{\psi}_{r\beta} - \tilde{i}_{s\beta}\hat{\psi}_{r\alpha} + k_c s_\omega\right), \tag{34}$$

where

$$s_\omega = \tilde{i}_{s\alpha}\hat{\psi}_{r\alpha} + \tilde{i}_{s\beta}\hat{\psi}_{r\beta}, \tag{35}$$

and

$$k_c = k_f \hat{\omega}_r, \qquad k_f > 0. \tag{36}$$

4. Method of speed estimation without an integrator structure

The adaptation mechanism according to [1, 3–5] and (34) requires the use of the integrator structure. Another approach to determine the value of the rotor speed can be the nonadaptive

mechanism. Considering the formula (28) it can be presented as a combination of two expressions:

$$\frac{\mathrm{d}\tilde{\omega}_r}{\mathrm{d}\tau} = -\gamma a_3 \Big(\underbrace{\tilde{i}_{s\alpha}\hat{\psi}_{r\beta}}_{I} - \underbrace{\tilde{i}_{s\beta}\hat{\psi}_{r\alpha}}_{II} \Big). \tag{37}$$

If individual expressions are considered separately, then this can define the following equations that should occur in these expressions, so that the observer structure is kept up with the object:

$$I: \qquad \tilde{i}_{s\alpha} \equiv \frac{1}{\gamma}\hat{\omega}_r \hat{\psi}_{r\beta}\,, \tag{38}$$

$$II: \qquad \tilde{i}_{s\beta} \equiv -\frac{1}{\gamma}\hat{\omega}_r \hat{\psi}_{r\alpha}\,. \tag{39}$$

In the next step, both sides of (34) and (35) should be multiplied by $\hat{\psi}_{r\beta}$ and $\hat{\psi}_{r\alpha}$, respectively, and added to each other and transformed so as to obtain the formula:

$$\hat{\omega}_r = \gamma \frac{\tilde{i}_{s\alpha}\hat{\psi}_{r\beta} - \tilde{i}_{s\beta}\hat{\psi}_{r\alpha}}{\hat{\psi}_r^2}\,. \tag{40}$$

After substitution of (40) for (37), assuming that $\dot{\omega}_r = 0$ the solution of equation (37) is:

$$\tilde{\omega}_r = \tilde{\omega}_{r0} e^{-\vartheta\tau}, \tag{41}$$

where

$$\hat{\psi}_r^2 = \hat{\psi}_{r\alpha}^2 + \hat{\psi}_{r\beta}^2\,.$$

In (41) it has been shown that for $\tau \to 0$, the rotor speed estimation error will exponentially decay to zero, with the order of convergence equal to $\vartheta = a_3\hat{\psi}_r^2$.

Proposition 3. In order to improve the properties of rotor angular speed estimation from (40), a feedback coupling should be introduced in a similar way as in (33), which is a scalar product of vectors. If (38) and (39) are multiplied by components $\hat{\psi}_{r\beta}$ and $\hat{\psi}_{r\alpha}$, respectively, and (38), (39) by $\hat{\psi}_{r\alpha}$ and $\hat{\psi}_{r\beta}$ then the following is obtained:

$$\tilde{i}_{s\alpha}\hat{\psi}_{r\beta} - \tilde{i}_{s\beta}\hat{\psi}_{r\alpha} \equiv \frac{1}{\gamma}\hat{\omega}_r \psi_r^2\,, \tag{42}$$

$$\tilde{i}_{s\alpha}\hat{\psi}_{r\alpha} + \tilde{i}_{s\beta}\hat{\psi}_{r\beta} \equiv 0. \tag{43}$$

By adding the terms (42) to (43) on both sides and after transformation, one obtains:

$$\hat{\omega}_r = \gamma \frac{\tilde{i}_{s\alpha}\hat{\psi}_{r\beta} - \tilde{i}_{s\beta}\hat{\psi}_{r\alpha} + k_c s_\omega}{\hat{\psi}_r^2}\,, \tag{44}$$

where

$$s_\omega = \tilde{i}_{s\alpha}\hat{\psi}_{r\alpha} + \tilde{i}_{s\beta}\hat{\psi}_{r\beta}\,, \tag{45}$$

and $\gamma = 1$ p.u.

The value of the rotor speed can be determined from the formula (40) from the proposed algebraic expression.

It is worth noting that if $\left(\frac{1}{2\gamma}\tilde{\omega}_r^2\right)$ is omitted in (24) (the function responsible for the adaptive speed reproduction mechanism), then the derivative form of the Lyapunov function is as follows:

$$\dot{V} = a_5\left(\tilde{\psi}_{r\alpha}^2 + \tilde{\psi}_{r\beta}^2\right) - \tilde{\omega}_r a_3\left(\hat{\psi}_{r\beta}\tilde{i}_{s\alpha} - \hat{\psi}_{r\alpha}\tilde{i}_{s\beta}\right) \le 0, \tag{46}$$

which with assumption $\dot{\omega}_r = 0$ confirms that Lyapunov theorem is satisfied and asymptotic stability of the system

$$\dot{V} = a_5\left(\tilde{\psi}_{r\alpha}^2 + \tilde{\psi}_{r\beta}^2\right) - \tilde{\omega}_r^2 a_3 \hat{\psi}_r^2 \le 0, \tag{47}$$

for $\hat{\psi}_r^2 > 0$.

The continuous function k_c occurring in (34) and (44) in some operating ranges of the machine (e.g. during zero speed and load torque changes) can be replaced by a discontinuous form depending on the reference speed value or vector product specified for vectors of stator voltage and rotor flux:

$$k_c = k_f \mathrm{sgn}(.) = \begin{cases} 1 & \left(u_{s\beta}\hat{i}_{s\alpha} - u_{s\alpha}\hat{i}_{s\beta}\right) < 0, \\ -1 & \left(u_{s\beta}\hat{i}_{s\alpha} - u_{s\alpha}\hat{i}_{s\beta}\right) \ge 0, \end{cases} \tag{48}$$

or

$$k_c = k_f \mathrm{sgn}(.) = \begin{cases} 1 & x_{11}^* < 0, \\ -1 & x_{11}^* \ge 0, \end{cases} \tag{49}$$

where x_{11}^* is the reference rotor speed.

It is worth noticing that in the experimental stand the introduced stabilizing function defined (35), (45) can be filtrated by the first order filter in order to minimize the unexpected oscillation or estimated rotor speed value which is used in the multi-scalar transformation.

5. Control system of induction machine

Proposed observer structure was tested in the closed-loop control system with the multi-scalar variables. The sensorless control structure is shown in Fig. 1. The multi-scalar variables were proposed in [17] and they are defined as follows:

$$x_{11} = \hat{\omega}_r\,, \tag{50}$$

$$x_{12} = \hat{\psi}_{r\alpha}\hat{i}_{s\beta} - \hat{\psi}_{r\beta}\hat{i}_{s\alpha}\,, \tag{51}$$

$$x_{21} = \hat{\psi}_{r\alpha}^2 + \hat{\psi}_{r\beta}^2\,, \tag{52}$$

$$x_{22} = \hat{\psi}_{r\alpha}\hat{i}_{s\alpha} + \hat{\psi}_{r\beta}\hat{i}_{s\beta}\,, \tag{53}$$

where $\hat{\omega}_r$ is the estimated rotor speed value, $\hat{i}_{s\alpha}$, $\hat{i}_{s\beta}$ are the estimated stator current vector components and $\hat{\psi}_{r\alpha}$, $\hat{\psi}_{r\beta}$ are the estimated rotor flux vector components.

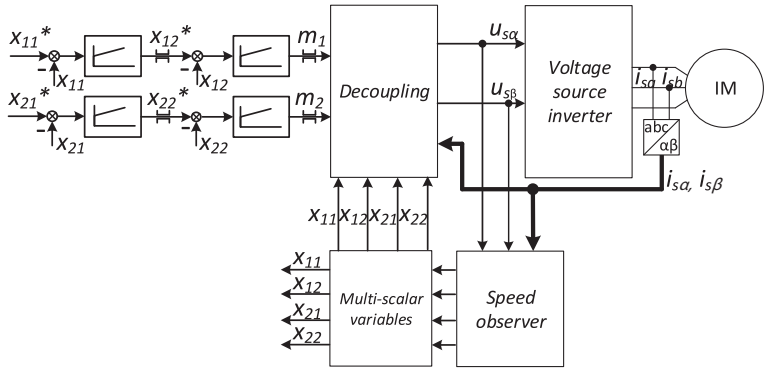

Fig. 1. Sensorless control structure with proposed speed observer and multi-scalar variables

Using the mathematical model of IM and taking into account multi-scalar transformation (50)–(53), the feedback linearizing control law (decoupling) was presented in [14, 17]. In Fig. 1 the control system structure is shown. The full description of the scheme presented in Fig. 1 is in [14, 17].

6. Simulation results

The theoretical issues presented in the previous sections were confirmed by the simulation. It was assumed that the sampling time was 150 μs, while the integration step of the induction machine model was 1 μs. The control system with the multi-scalar variables is shown in Fig. 1. There are the following blocks: multi-scalar variables, decoupling, and speed observer. The reference values (inputs) are the rotor speed and the square of the rotor flux.

Fig. 2 shows the waveforms of multi-scalar variables (50)–(53) and the error of the estimated rotor speed during changes of reference speed and load torque. At 0.7 s, the reference speed was changed from 0.1 to 0.95 p.u. after 1.5 s from 0.95 to −0.95, while after 2.5 s the load torque value was set to 0.75 p.u. The speed was estimated from (28).

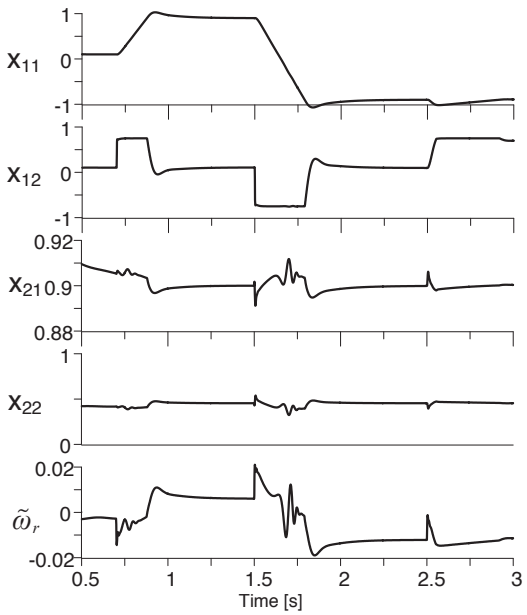

Fig. 2. Waveforms of multi-scalar variables and $\tilde{\omega}_r$ during changes in the reference speed (x_{11}^*) in the range from 0.95 to −0.95 and the load torque from 0.1 to 0.75 p.u., speed is estimated from (28)

In Fig. 3 the rotor speed is reconstructed from (34). In addition to the multi-scalar variables, s_ω function is presented. If the rotor speed is estimated from (34) (by using s_ω function), the rotor speed error has a smaller value than in Fig. 2.

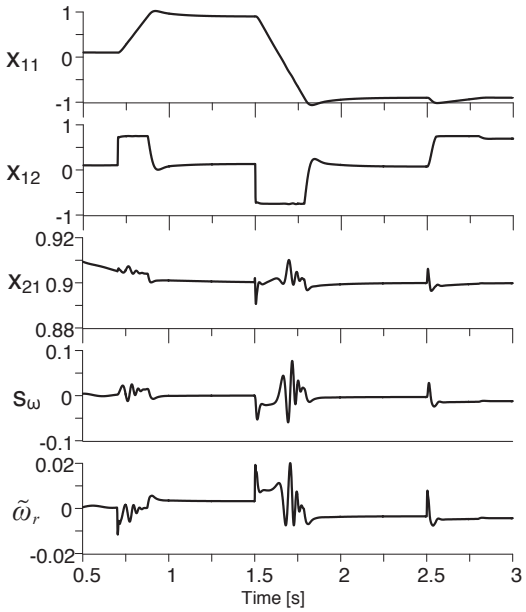

Fig. 3. Waveforms of multi-scalar variables and $\tilde{\omega}_r$ during changes in the reference speed (x_{11}^*) in the range from 0.95 to −0.95 and the load torque from 0.1 to 0.75 p.u., speed is estimated from (34)

Figs. 4 and 5 present the changes of IM working modes. The load torque is changed from 0 to 0.9 p.u. and from 0.9 to −0.9 p.u., the rotor speed was set to 0.08 p.u. In Fig. 4 the speed is reproduced from (28), and in Fig. 5 from (34), using function (35). For motor operation, the load torque value was 0.9 p.u., while for generator operation −0.9 p.u. The rotor speed error is increased during the regenerating IM mode (Fig. 4), but while the speed is estimated from (34), the rotor speed error is near zero (Fig. 5). Introduced to the speed adaptation mechanism

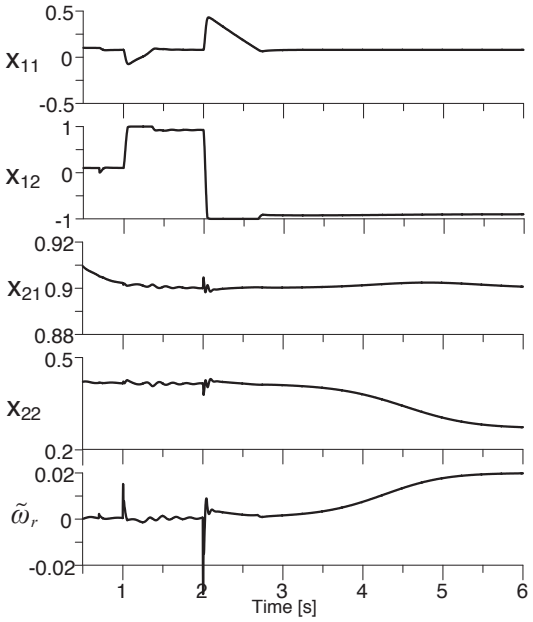

Fig. 4. Waveforms of multi-scalar variables during load torque changes from 0.9 to −0.9 p.u., speed value is determined from (28)

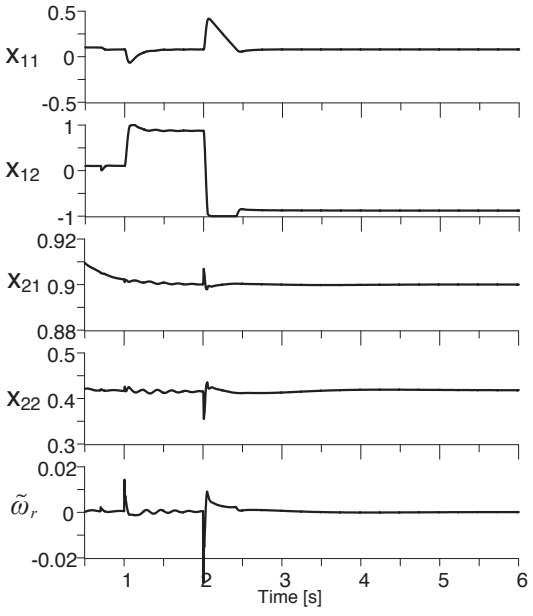

Fig. 5. Waveforms of multi-scalar variables during load torque changes from 0.9 to −0.9 p.u., speed value is determined from (34)

proposed s_ω function in (35) reduces the speed estimation error to zero during the load torque injection in regenerating mode. After 2 s the load torque is injected and in Fig. 4 the rotor speed error increases above 0.02 p.u. for $k_c = 0$, if $k_c \neq 0$, the rotor estimation error does not change value which is presented in Fig. 5.

In Figs. 4 and 5 x_{12} was limited to 1.0, therefore in x_{11} long response is visible during the load torque, changing to −0.9 p.u. In Fig. 5 this response takes less time because of using the proposed robust speed estimation law (34). The waveforms from Figs. 2–5 confirm the theoretical assumptions presented in Proposal 2 on increasing the robustness of the speed observer structure on a disturbance.

7. Experimental results

Experimental tests were conducted on a 5.5 kW IM supplied by voltage source inverter (as shown in Fig. 13). Drive system parameters are shown in Table 1.

Table 1
Nominal and base parameters of IM

Name	Description	Value
P_n	Nominal power	5.5 kW
I_n	Stator current (Y)	11 A
U_n	Stator voltage (Y)	400 V
n	Nominal speed	1430 rpm
f	Frequency	50 Hz
$U_b = U_n$	Base voltage	400 V
$I_b = I_n\sqrt{3}$	Base current	18.9 A
P_b	Base power	7.56 kW
R_{sN}	Stator resistance	0.035 p.u.
R_{rN}	Rotor resistance	0.035 p.u.
L_{mN}	Magnetizing inductance	1.95 p.u.
$L_{s,rN}$	Stator and rotor inductance	2.05 p.u.

The experimental tests were divided into three sections: 7.1 Machine start-up and reverse, 7.2 Motor and regenerating modes and 7.3 Uncertainty of nominal parameters.

7.1. Machine start-up and reverse. Fig. 6 shows the waveforms of multi-scalar variables and the square of the stator

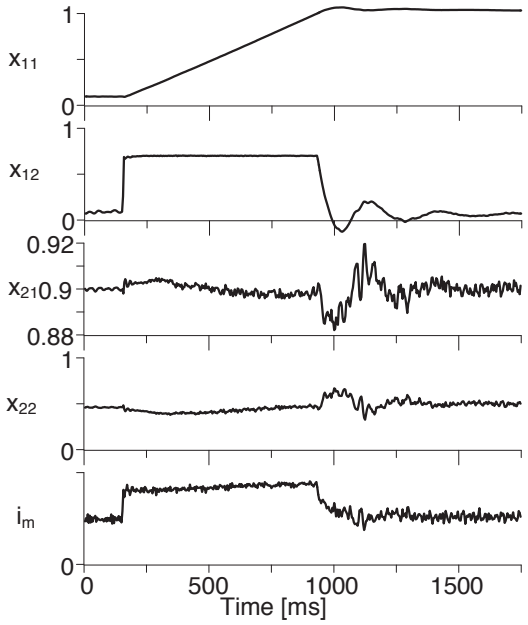

Fig. 6. Machine starting up to 1.0 p.u. – the speed is reproduced from the adaptive relationship (34)

current vector during start-up to the speed of 1.0 p.u. The rotor speed is reproduced from the adaptive dependence (34). In Fig. 7 the same variables are presented during the IM start-up to 1.0 p.u. but the rotor speed is estimated nonadaptively from (44).

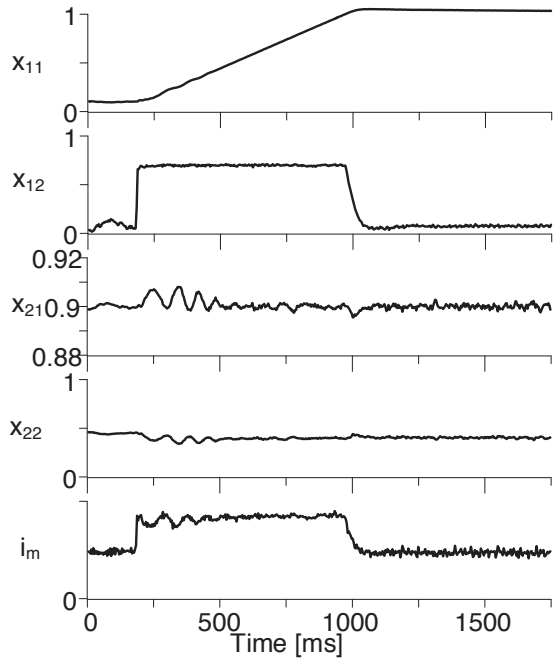

Fig. 7. Machine starting up to 1.0 p.u. – the speed is reproduced nonadaptively from (44)

Fig. 8 shows the waveforms of multi-scalar variables and the square of the stator current vector during the IM reversal to

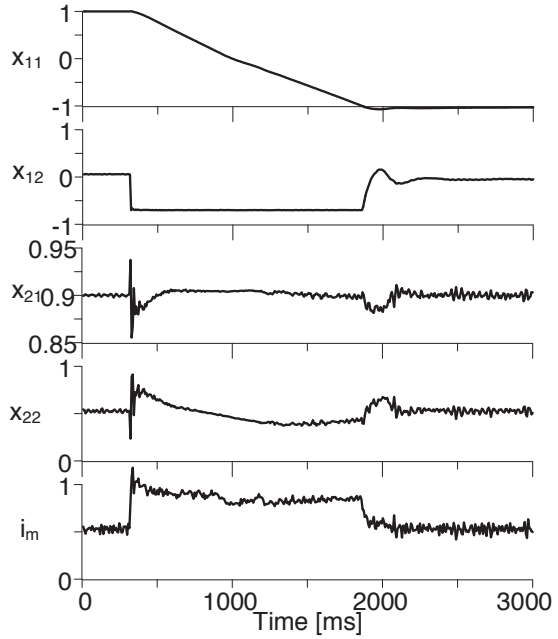

Fig. 8. Reverse from 1.0 to −1.0 p.u. – the rotor speed is estimated from the adaptive dependence (34)

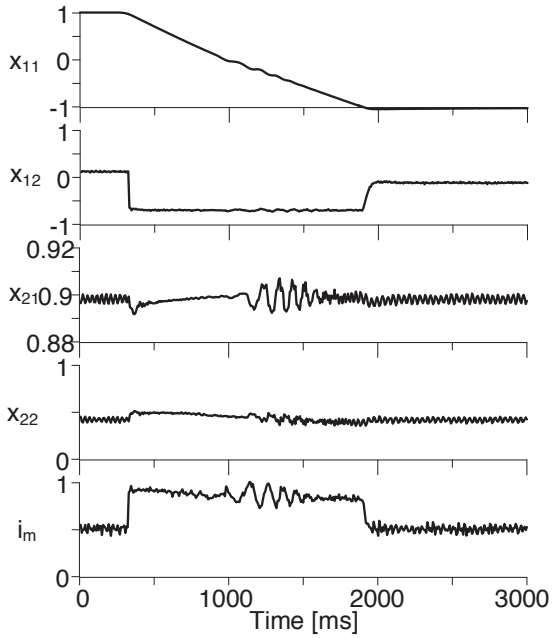

Fig. 9. Reverse from 0.95 to −0.95 p.u. – the rotor speed is estimated from the nonadaptive dependence (44)

−1.0 p.u., for the rotor speed value determined from adaptive dependence (34). In Fig. 9 the rotor speed is estimated nonadaptively from (44). In the case presented in Fig. 9, oscillations of the presented values during the zero crossing are visible, which have a lower value for the case from Fig. 8. The reason for these oscillations (Fig. 9) visible in the rotor speed and x_{21} transients is noncontinuous signum function defined in (48).

In Fig. 10 the waveforms of estimated rotor flux vector, stator current vector components and speed estimation error during

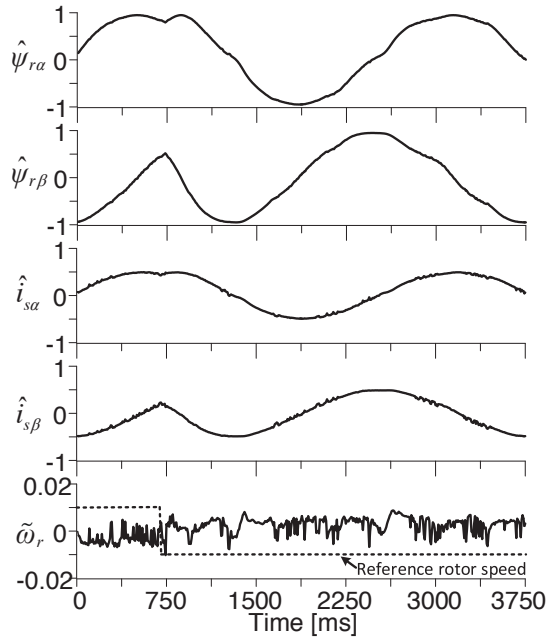

Fig. 10. Waveforms of state estimation during the rotor speed reverse from 0.01 to −0.01 p.u. – the rotor speed is estimated nonadaptively

the IM reverse from 0.01 to −0.01 p.u. are shown. The rotor speed error is smaller than 0.01 p.u.

7.2. Motor and regenerating mode. In Figs. 11 and 12 the waveforms of multi-scalar variables and the square of the stator current vector in terms of motor and generator operation are shown.

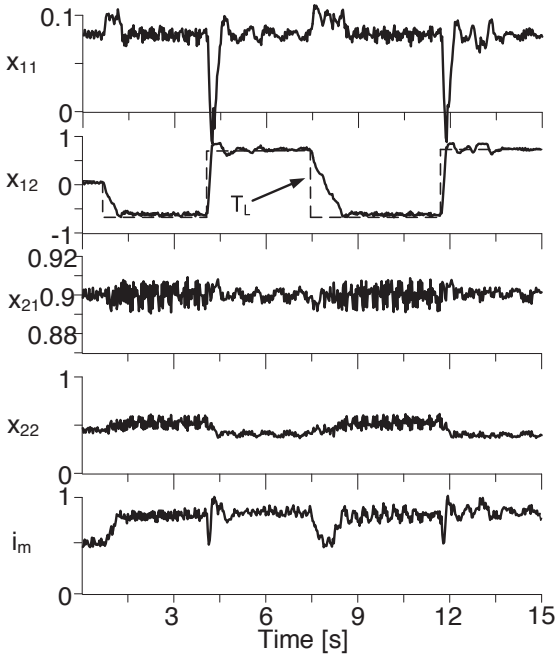

Fig. 11. Load torque is changed, the rotor speed is reproduced from proposed adaptive robust law (34)

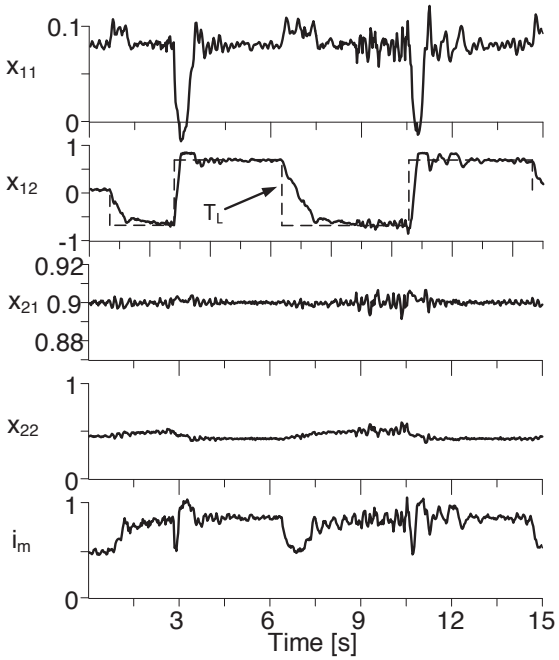

Fig. 12. Load torque is changed, the rotor speed is reproduced non-adaptively (44)

The reference speed is 0.08 p.u. The load torque value was changed in the range of 0.7 to −0.7 p.u. Fig. 11 presents the waveforms for the case in which the value of the rotor speed was reproduced from the robust adaptation law proposed in (34), while in Fig. 12 – the nonadaptive method of speed estimation (44). In the case presented in Fig. 11, oscillations of variables x_{21} and x_{22} during generator operation are visible (the load torque is about $T_L = -0.7$ p.u.). These oscillations are caused by the tuning gain above $\gamma = 0.1$ p.u. in the integrator structure (34). The waveforms from Fig. 12 do not contain such a level of the oscillation like in Fig. 11 $(x_{21},\ x_{22})$.

7.3. Uncertainty of nominal parameters. In this section the nominal parameters of IM (stator and rotor resistances) are detuned. Because of that the behaviour of AFO structure is independent of the speed estimation mechanism, the uncertainties tests are conducted only for a nonadaptive case.

In Fig. 13, after 0.5 s the stator resistance is changed from 0.035 to 0.1 $(R_s = 2.85R_{sN})$. The rotor speed estimation error increases to about 0.015–0.02 p.u. The AFO structure errors are strongly dependable on the value of rotor resistance.

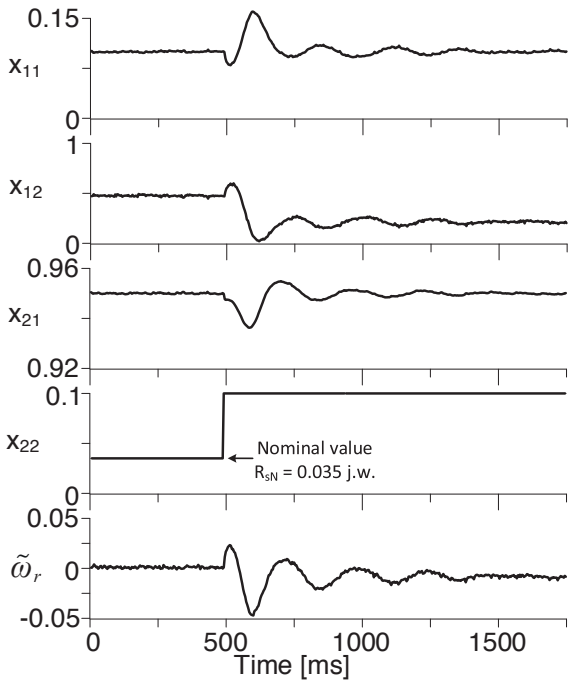

Fig. 13. After 500 ms the nominal value of stator resistance is changed up to 0.1 p.u., the rotor speed is reproduced nonadaptively (44), machine is loaded about 0.5 p.u.

In Fig. 14 the rotor resistance is changed from 0.035 to 0.1 p.u. $(R_r = 2.85R_{rN})$. The rotor speed estimation error increases to about 0.03 p.u. Despite the speed error the x_{12} value is on the same level (about 0.5 p.u.)

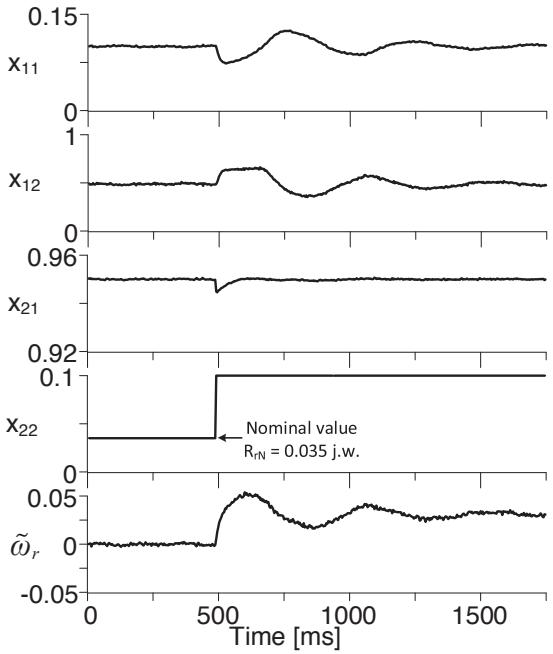

Fig. 14. After 500 ms the nominal value of rotor resistance is changed up to 0.1 p.u., the rotor speed is reproduced nonadaptively (44), machine is loaded about 0.5 p.u.

8. Conclusions

The paper presents the synthesis of the rotor speed observer estimation of the IM. A modification of the classic adaptation law has been proposed, from which the speed value is reproduced, thus enabling an increase in the range of stable drive operation in the motor and generator range at speeds lower than 0.1 p.u. In addition, a nonadaptive method of reproducing the value of the rotor speed has been proposed, which facilitates a stable operation of the machine in the adopted operating ranges. Considering theoretical and experimental investigations, the following conclusions can be drawn:

- Introducing an additional coupling in the integrator structure ensures stable operation in the considered range of changes in rotor angular speed and load torque.
- The proposed "new" method of reproducing the rotor speed from algebraic dependence allows stable operation in the considered range of changes in rotor speed and load torque.
- The proposed method of introducing additional coupling (for both adaptive and nonadaptive law) allows stable operation in the motor mode, at zero speeds and in the regeneration mode and rated load torque.
- The steady-state error of estimated rotor speed did not exceed about 0.01 p.u. (in the experimental setup).

Theoretical assumptions were confirmed by experimental research.

References

[1] T. Orlowska-Kowalska, M. Korzonek, and G. Tarchała, "Stability analysis of selected speed estimators for induction motor drive in regenerating mode – A comparative study", *IEEE Trans. Ind. Electron.* 62 (10), 7721–7730 (2017).

[2] T. Orlowska-Kowalska, "Application of the extended luenberger observer for flux and rotor time constant estimation in induction motor drives", *IEE Proc.* 136, 324–330 (2006).

[3] H. Kubota, K. Matsuse, and T. Nakano, "DSP-based speed adaptive flux observer of induction motor", *IEEE Trans. Appl. Ind.* 29, 344–348 (1993).

[4] M. Hinkkanen and J. Luomi, "Stabilization of regenerating-mode operation in sensorless induction motor drives by full-order flux observer design", *IEEE Trans. Ind. Electron.* 51 (6), 1318–1328 (2004).

[5] Ch. Luo, B. Wang, Y. Yu, Ch. Chen, Z. Huo, and D. Xu, "Operating-point tracking method for sensorless induction motor stability enhancement in low-speed regenerating mode", *IEEE Trans. Ind. Electron.* 67 (5), 3386–3397 (2020).

[6] K. Szabat, T. Orlowska-Kowalska, and K.P. Dyrcz, "Extended Kalman filters in the control structure of two-mass drive system", *Bull. Pol. Ac.: Tech.* 54 (3), 315–325 (2006).

[7] M. Comanescu, "Design and implementation of a highly robust sensorless sliding mode observer for the flux magnitude of the induction motor", *IEEE Trans. Energy Convers.* 31 (2), 649–657 (2016).

[8] M. Morawiec and A. Lewicki, "Application of sliding switching functions in backstepping based speed observer of induction machine", *IEEE Trans. Ind. Electron.* 67 (7), 5843–5853 (2020).

[9] P. Serkies, "Estimation of state variables of the drive system with elastic joint using moving horizon estimation (MHE)", *Bull. Pol. Ac.: Tech.* 67 (5), 883–892 (2019).

[10] C. Schauder, "Adaptive speed identification for vector control of induction motors without rotational transducers", *IEEE Trans. Ind. Appl.* 28 (5), 1054–1061 (1992).

[11] T. Białoń, A. Lewicki, M. Pasko, and R. Niestrój, "PI observer stability and application in an induction motor control system", *Bull. Pol. Ac.: Tech.* 61 (3), 595–598 (2013).

[12] Z. Krzeminski, "A new speed observer for control system of induction motor", in *IEEE Int. Conference on Power Electronics and Drive Systems, PESC'99*, Hong Kong, 1999.

[13] Z. Krzeminski, "Obserwatory prędkości dla bezczujnikowego sterowania maszynami prądu przemiennego", *Prz. Elektrotechniczny* R. 90 (5), 1–7 (2014) [in Polish].

[14] M. Morawiec, "Z type observer backstepping for induction machines", *IEEE Trans. Ind. Electron.* 62 (4), 2090–2103 (2015).

[15] T. Orlowska-Kowalska, M. Korzonek, and G. Tarchała, "Stability improvement methods of the adaptive full-order observer for sensorless induction motor drive – Comparative study", *IEEE Trans. Ind. Inf.* 15 (11), 6114–6126 (2019).

[16] J.J. Listwan, "Analysis of fault states in drive systems with multiphase induction motors", *Arch. Electr. Eng.* 68 (4), 817–830 (2019).

[17] Z. Krzeminski, "Nonlinear control of induction motor", in *10th IFAC World Congress*, Munich, 1987.

[18] P. Ioannou and J. Sun, *Robust Adaptive Control*, Prentice Hall, USA, 1996.

[19] L. Jarzebowicz, "Error analysis of calculating average d-q current components using regular sampling and park transformation in FOC drives", in *Proc. 2014 (EPE)*, 2014.